

AD P000920

MAGNETOSTATIC FORWARD VOLUME WAVE DEVICES*

J. D. Adam, Michael R. Daniel and T. W. O'Keeffe
Westinghouse Electric Corporation, Research & Development Center
Pittsburgh, PA 15235

Summary

The design, construction and performance of four magnetostatic wave devices operating at X-band is described. They comprise a dispersive delay line with a 1 GHz bandwidth and a differential delay of ~ 200 nS, a programmable tapped delay line capable of generating and correlating 4-bit Barker codes, a delay stabilized oscillator with output frequency stable to within ± 1 MHz over the 0 to $+65^\circ\text{C}$ range and a 10-channel filter bank.

Introduction

Magnetostatic wave (MSW) devices, based on epitaxial YIG are potentially useful for signal processing at microwave signal frequencies or at a broadband microwave i.f. MSW are attractive because of their low propagation losses of less than 30 dB/ μS at microwave frequencies and their planar geometry and bandwidths of the order of 1 GHz are compatible with presently available semiconductor amplifiers or signal sources. The objective here is to describe four types of devices developed and delivered on a U.S. Air Force Avionics Lab. program.¹ The devices were a dispersive delay line, a delay stabilized oscillator, a programmable tapped delay line and a 10-channel filter bank, all operating in X-band. These devices were all packaged with permanent bias magnets with the aim of allowing potential users to evaluate and gain experience with MSW devices and provide feedback on areas requiring further development. The device types were selected since these functions are currently performed by SAW devices operating at i.f. frequencies below 1 GHz.

The forward volume mode of propagation was used in all of the devices. This mode was chosen since the dispersive delay line required a bandwidth of 1 GHz at X-band which would be impossible to achieve with a simple surface wave device. In addition, although forward volume wave

*Supported by the U.S. Air Force Avionics Laboratory under Contract No. F33615-77-C-1068.

require a larger bias field than either surface or backward volume waves, the field is applied normal to the YIG film, thus minimizing the magnet gap. Device design and fabrication relied where possible on simple transducer structures and the use of adjacent ground planes to achieve the desired delay characteristics. Equations describing FVW propagation and transduction in structures consisting of a YIG film spaced from a ground plane have been described elsewhere^{2,3} and will not be discussed in detail at this time.

Dispersive Delay Line

The desired delay versus frequency characteristics of the dispersive delay line were obtained by taking advantage of the strong influence of an adjacent conducting plane on the wave dispersion. Studies⁴ showed that an approximately linear variation of group delay with frequency was obtained when the ground plane was spaced from the YIG film by a distance approximately equal to the YIG film thickness. A nominally 20 μ m YIG thickness was selected as giving a reasonable time bandwidth product of ~ 200 at a bandwidth of 1GHz with a deviation from linear delay with frequency of less than ± 5 nS.

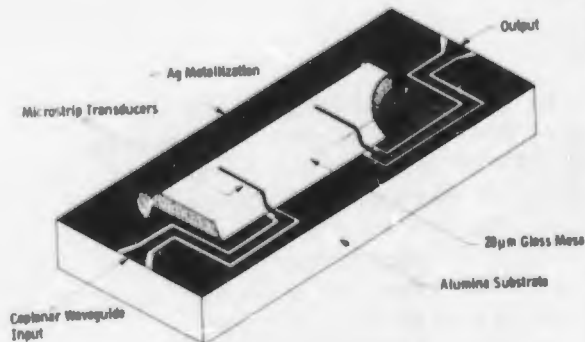


Figure 1. Transducer and dielectric spacer configuration for the linearly dispersive delay line.

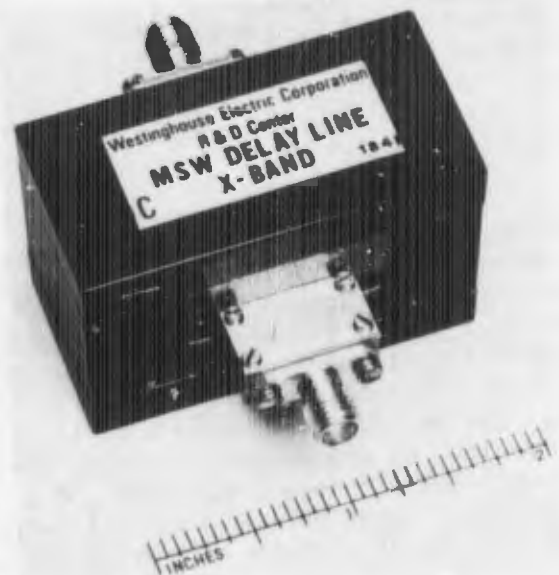


Figure 2. Linearly dispersive delay line.

The construction of the device is shown in figure 1, where the YIG film of dimensions 5mm x 25mm x 20 μ m would be placed face down on the glass mesa so as to contact the microstrip transducers. The glass mesa was deposited on the gold ground plane by sputtering. The

gold microstrip transducers were 5mm long, 50 μ m wide and 5 μ m thick and were open circuited at one end with the opposite end connected to co-planar waveguide of 50 Ω characteristic impedance. The packaged device is shown in figure 2 complete with the SmCo permanent magnets and soft iron yoke required to supply the 4.8 kOe bias field.

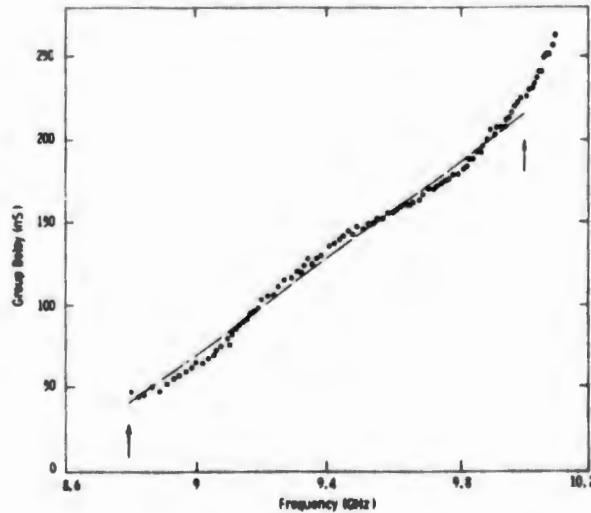


Figure 3. Measured group delay vs. frequency for the linearly dispersive delay line.

with calculated curves which include the effects of the finite resistivity of the conducting plane on the propagation loss. Two cases were calculated,¹ the first assumed a silver conducting layer with a skin depth of 0.6 μ m

The variation in group delay with frequency is shown in figure 3. The dots are measured points and the broken line is a best fit straight line. Arrows denote the 1.2 GHz bandwidth over which the delay is linear with frequency to within ± 5 nS and the differential delay is 190nS. Phase deviation from quadratic phase with frequency is a more sensitive parameter than deviation from linear delay with frequency. The maximum phase deviation for the device shown is approximately 240° which will require to be reduced by at least an order of magnitude to satisfy most applications.

The measured insertion loss is shown in figure 4, together

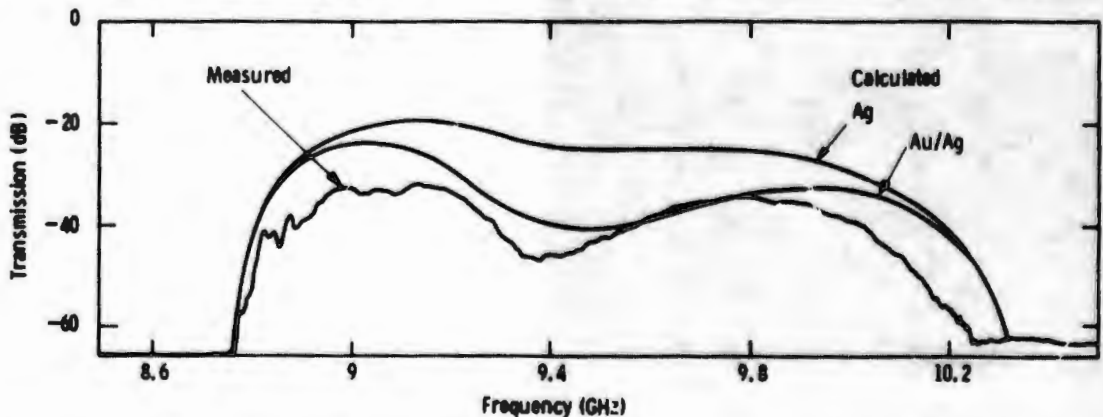


Figure 4. Transmission loss vs. frequency for the linearly dispersive delay line.

at 9 GHz and the second a gold/silver alloy with a skin depth of 2 μ m. The measurements are in good agreement with the latter case since in this device a thin gold film was used to passivate a thick silver layer resulting in a gold/silver alloy by diffusion.

Providing the phase error of the dispersive delay lines can be reduced they will find important applications in compressive receivers and in variable delay lines for phased array antennas.⁵ This progress is likely owing to the number of more sophisticated techniques such as double YIG film⁶ and reflective array devices which have not yet been fully developed.

Programmable Tapped Delay Line

The device discussed in this section is a programmable tapped delay line⁷ which can be used to generate and correlate a phase coded pulse sequence. The 4-tap device is shown in Figure 5. The YIG film is the dark strip towards the bottom of the photograph and is 7.1 μ m thick, 2cm long and 1mm wide. The input transducer is at the bottom center and the four output taps are arranged two on either side of the input and successive output taps. The taps are connected via 100 Ω microstrip to PIN diode, 0 or π , phase shifters and then combined together. The microstrip circuit was fabricated on a 10 mil thick alumina substrate, 1" square. Switching and bias inputs for the PIN switches can be seen on both sides of the box. When completely assembled, the field produced by the permanent bias magnets was normal to the film. The insertion loss from the input to any output was typically 22dB.

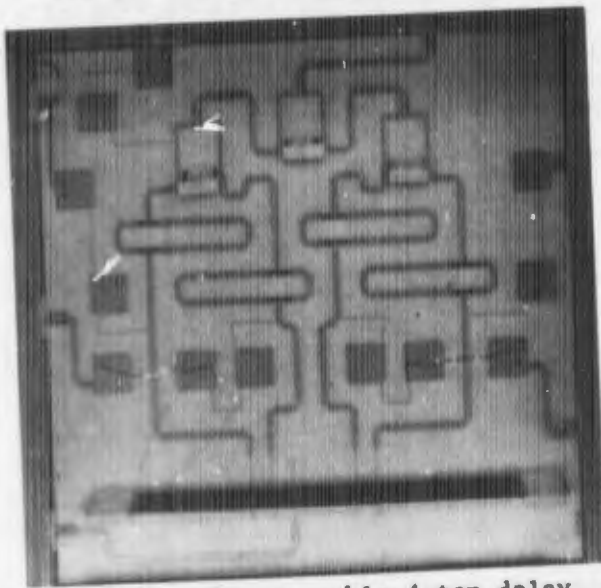


Figure 5. Programmable 4-tap delay line.

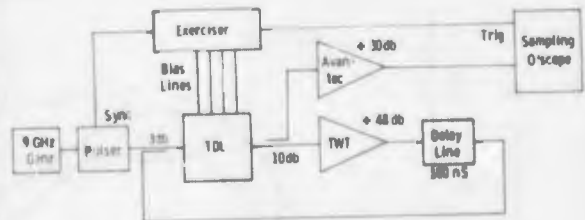


Figure 6. Tapped delay line test arrangement.

The tapped delay line was tested by using the same device to generate and then correlate a 4-bit Barker code, Figure 6. A 9 GHz pulse of length 20nsec was applied to the input transducer resulting in a phase coded train of four pulses from the output of the tapped

delay line. The phase coded pulses were delayed for 100nsec in a constant MSW delay line and during this time the phase of the four taps was changed by an exerciser so as to represent a time reversed version of the generated pulse train. The pulse train was then amplified and reintroduced to the input of the tapped delay line via a directional coupler. The tapped delay line acted as a matched filter and performed a correlation on the four coded pulses. The sequence of pulses observed at the output to the tapped delay line is shown in Figure 7. Feedthrough from the input pulse is seen on the extreme left followed by the four generated pulses which are coded with the $\pi, \pi, 0, \pi$ Barker code. The correlation peak is seen towards the right of the photo. For this 4-bit Barker code the correlation is a 7 pulse sequence with normalized amplitudes 1, 0, 1, 4, 1, 0, 1. The experimental results are in good agreement with this although some extra undesired pulses are evident which are due to reflections and higher order width modes.

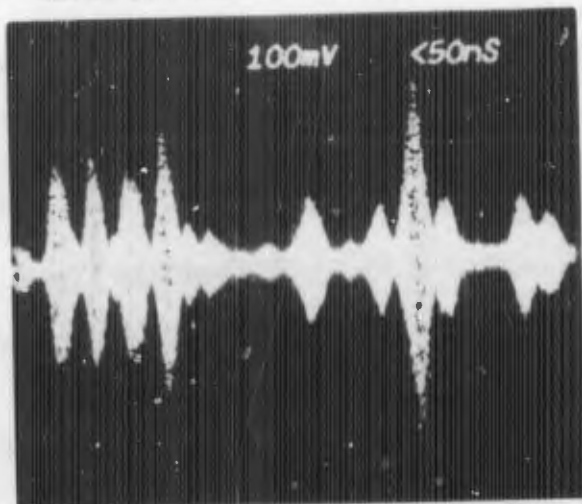


Figure 7. 4-bit Barker code generation and correlation.

Generation and correlation using two separate devices was less successful due to difficulty in matching the characteristics of the devices with sufficient accuracy. The main problem lay in achieving sufficient bias field uniformity since an 0.5 Oe change in bias field was sufficient to produce an 10° phase change between taps. This problem will be minimized with improved magnet design. The techniques described are capable of extension to the generation and correlation of 13-bit Barker codes as well as other sequences for use in radar and communications systems.

Delay Stabilized Oscillator

An important goal in the design of this oscillator was that the variation in output frequency as a function of temperature be at least as good as commercially available YIG sphere oscillators which is typically less than 10MHz over 0°C to $+60^\circ\text{C}$.⁸ The frequency stability achieved with the MSW devices was $\pm 1\text{MHz}$ over the same temperature range with no internal heater. In epitaxial YIG devices the center frequency depends upon the temperature variation of both the $4\pi\text{M}$ and the anisotropy field (H_A). Techniques which were previously described and achieved temperature stable operation relied either on a special $\text{Y}_{3-x}\text{La}_x\text{Fe}_{5-y}\text{Ga}_y\text{O}_{12}$ film composition⁹ or used a separate temperature stabilizing component in the permanent magnet assembly. In the device described here, the frequency drift was minimized by designing the permanent bias magnet to compensate for the variation of the YIG film parameters, $4\pi\text{M}$ and H_A , with temperature.

Both periodic transducers and reflective arrays¹⁰ have been used in MSW oscillators. However, the present device was designed as a MSW analogue to a SAW delay stabilized oscillator. Figure 8a is a diagram of a delay stabilized oscillator consisting of an amplifier and an attenuator to provide controlled loop gain, a directional coupler to extract the signal from the oscillator and the delay line. If the delay line and other components in the loop are broadband, then oscillation will occur at any frequency where the total phase change around the loop is $2n\pi$ radians. The possible "comb" of frequencies is shown in Figure 8b. If the delay line is made narrow band, through the use of IDTs for example, then one frequency can be selected from the "comb" as shown by the broken line in Figure 8b. The situation shown here is ideal since the desired frequency is positioned at the maximum of the delay line amplitude response while other "comb" frequencies are positioned at zeros. This was achieved, as shown in Figure 9, by using a long IDT¹¹ (10 fingers) and a short IDT (4 fingers).

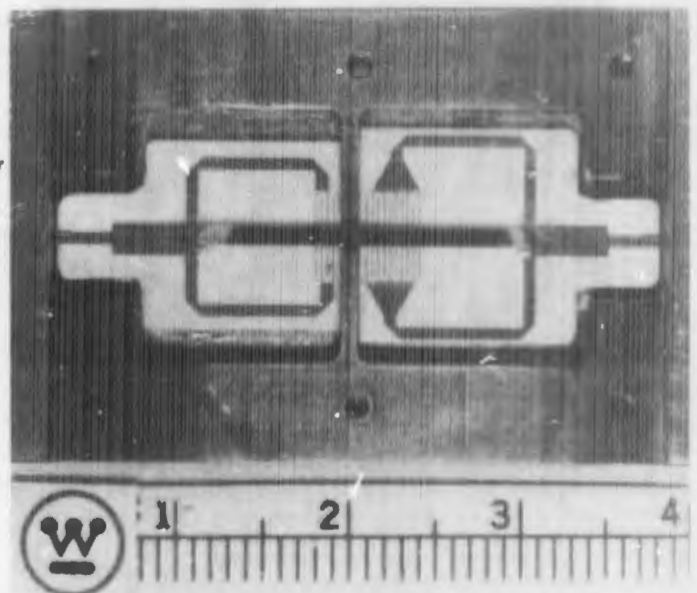
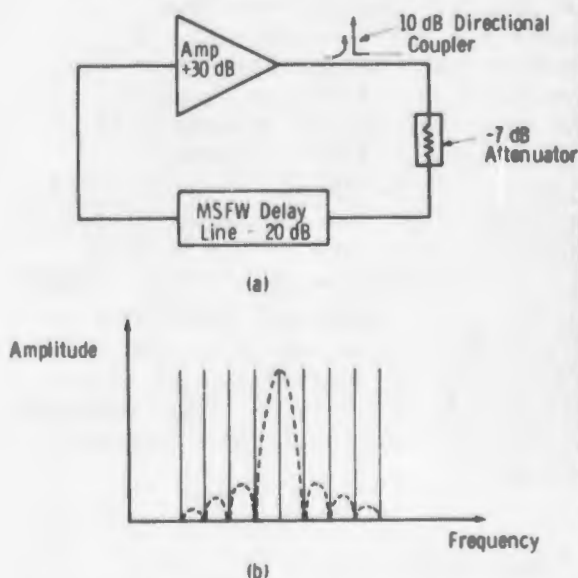


Figure 8. Magnetostatic wave delay stabilized oscillator: a) oscillator loop; b) selection of one oscillation mode by IDT response.

Figure 9. Magnetostatic forward volume wave delay line with IDTs for oscillator.

Ideally the center to center spacing of the transducers should equal the length of the longer transducer which was 3mm. The actual separation between the transducers was 4mm and was necessary to reduce e.m. feedthrough between input and output to less than 50dB. The additional separation did not seriously affect the rejection of other "comb" frequencies which were found to be attenuated by at least 14dB relative to the desired frequency where the minimum insertion loss was 19dB. Both transducers had fingers which were 5mm long and 50 μ m wide separated by 300 μ m. The YIG film was 7 μ m thick and, in order to reduce the coupling

to the transducer was made 1mm wide and spaced 75 μ m from it. The ends of the film were bevelled at $\sim 1/2^\circ$ to prevent reflections. The bias field was applied normal to the film so that MSFW were launched.

Measurements of the temperature dependence of the center frequency of the delay line, in a constant bias field, showed the frequency increased by +9MHz/ $^\circ$ C. This frequency change corresponds to a variation in internal field of +3.2 Oe/ $^\circ$ C. In order to achieve zero frequency change with temperature, this variation in internal field was compensated by an equal but opposite change in the bias field. For a device operating at 9GHz the required bias field change is approximately 0.065/ $^\circ$ C. The two materials considered in the construction of the bias magnets were SmCo and RARENET-B¹² with temperature coefficients of remanence of -0.04/ $^\circ$ C and -0.09/ $^\circ$ C respectively. A combination of these two materials were used to achieve the required behavior. Bias field uniformity over the length of the delay line is critical when IDTs are used and soft iron pole pieces were added to give a field uniform to less than 1 Oe over the active device area.



Figure 10. Delay line stabilized oscillator.

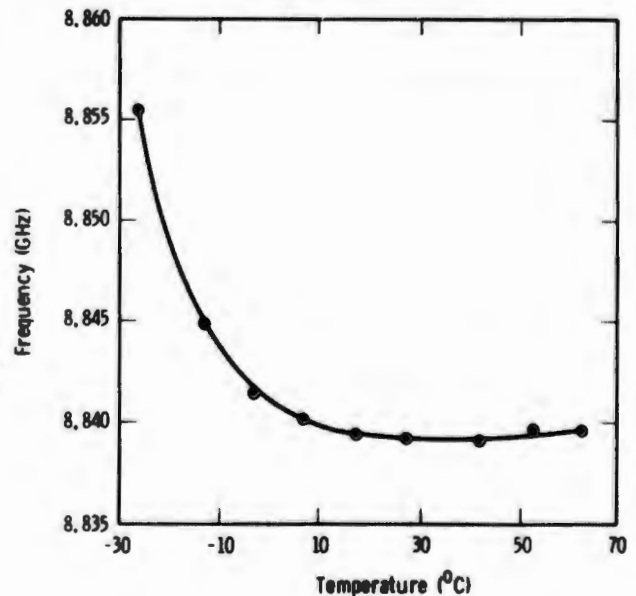


Figure 11. Variation in frequency of the delay stabilized oscillator as a function of temperature.

The assembled oscillator is shown in Figure 10. An amplifier having nominally 30dB gain over the range 7-12GHz was used. The open loop transmission amplitude and phase response was measured and the length of the semi-rigid coax and the attenuator values adjusted to give a net loop gain of +3dB with a phase change of 2π at 8.84GHz which was the center frequency of the delay line. The variation in center frequency of

oscillator with temperature is shown in Figure 11 over the range -30°C to $+70^{\circ}\text{C}$. The frequency is stable to within $\pm 1\text{MHz}$ over the range $+0^{\circ}\text{C}$ to $+65^{\circ}\text{C}$. At lower temperatures the frequency increases more rapidly with decreasing temperature. A similar increase in frequency with temperature is expected above the range shown here. This occurs because the variation of $4\pi m$ and anisotropy field are not linear functions of temperature.

Output power from the oscillator increased from $+7.6\text{dBm}$ at $+60^{\circ}\text{C}$ to $+9.8\text{dBm}$ at -20°C . Noise measurements were not performed but the effective Q , determined from the delay time (τ) by $Q = 2\pi f\tau$ was 5000. This Q value will be degraded by amplifier noise contributions. Although tuning using a coil wound on the bias magnet was not attempted, the low variation in oscillator frequency with temperature should be maintained. However the phase change with frequency which occurs in the loop external to the delay line would limit the tuning frequency range.¹⁰

10 - Channel Filter

The aim of the work described here was to design, fabricate and test a 10-channel multiplexed filter bank having minimum dispersion with 50MHz bandwidth channels contiguous at their 3dB points. The performance goals for the filter bank were:

Center frequency	9.0GHz
Number of Channels	10
Channel 3dB bandwidth	50MHz
Out of band rejection	55dB
50dB bandwidth	100MHz
Multiplexed insertion loss	20dB
Bandpass ripple	1dB

The filter bank was designed as 10 narrow band delay lines, each fed from a common input transducer but with separate output transducers, as show in Figure 12. A bias field gradient was applied along the device so that each delay line experienced a different bias field and hence had a different center frequency. The transducers were formed from 50Ω impedance microstrip line on 0.635mm thick alumina and were open circuited at the end. The position of the delay lines along the input transducer was such that each was close to $(N-\frac{1}{2})$ electromagnetic half wave lengths from the open circuited end at its center frequency.

Narrow band pass characteristics were obtained by use of wide transducers (0.635mm) spaced $160\mu\text{m}$ from the YIG surface. The measured

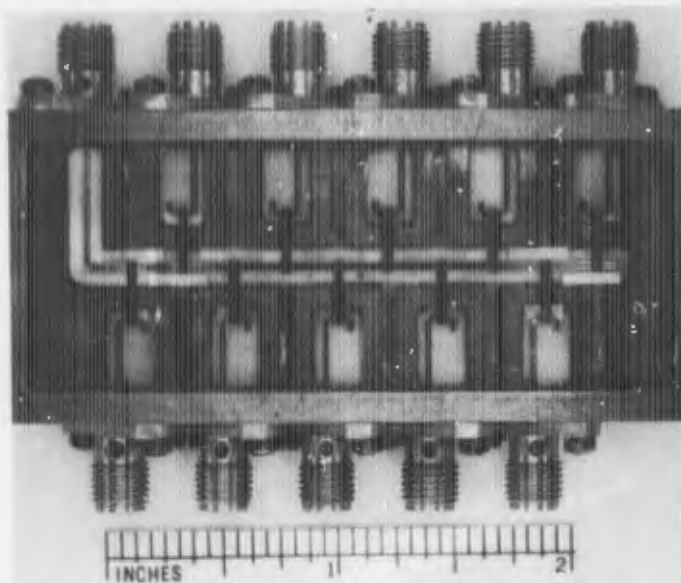


Figure 12. Interior of 10-channel filter bank.

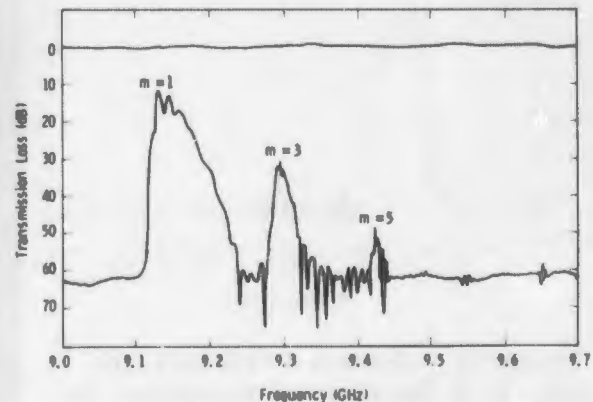


Figure 13. Measured transmission loss as a function of frequency for an 18.6 μm thick YIG film, 1 mm wide, spaced 160 μm from 5 mm long by 0.635 mm wide transducers.

transmission loss as a function of frequency for an 18.6 μm thick YIG film of width 1 mm is shown in figure 13. In this test, both transducers were 5 mm long, and 0.635 mm wide on 0.635 mm thick alumina. The YIG film was spaced from the transducer by 160 μm and the applied bias field was 4880 Oe. In common with the other devices, the ends of the YIG were bevelled at a $\frac{1}{2}^\circ$ angle to prevent reflections. Three separate peaks labelled $m = 1, 3,$ and 5 are clearly resolved. These correspond to width modes with transverse wave number $k = \frac{\pi}{W}, \frac{3\pi}{W}$ and $\frac{5\pi}{W}$, respectively. The behavior of width modes is discussed in more detail in a separate paper¹³ and will not be dwelt on here. Note that the $m = 1$ mode shows characteristics which approximate the bandwidth goals for this device.

Techniques to suppress the effects of the higher order width modes were investigated¹³ and it was found that the most effective approach in this configuration was an array of thin aluminum strips evaporated onto the surface of the YIG with the strips normal to the propagation direction. Eighteen strips of 300 \AA thick aluminum each 0.14 mm wide and separated by 0.13 mm resulted in attenuation of the $m = 3$ mode by 30 dB. The aluminum strips also produced a small but undesirable, ~ 2 dB, attenuation on the $m = 1$ mode. In order to compensate for the increased attenuation and also to improve the symmetry of the passband, the ends of the YIG were cut parallel to the transducers. The distance from the end of the YIG to the transducer was adjusted to give constructive interference of the waves at mid-band. Figure 14 shows the transmission loss, over a 1 cm path length, as a function of frequency measured on an 18.5 μm thick YIG film. This YIG film had 18 evaporated aluminum strips 364 \AA thick, to attenuate higher order width modes, and reflecting ends. The spacing from the ends of the film to the edge of the transducer was

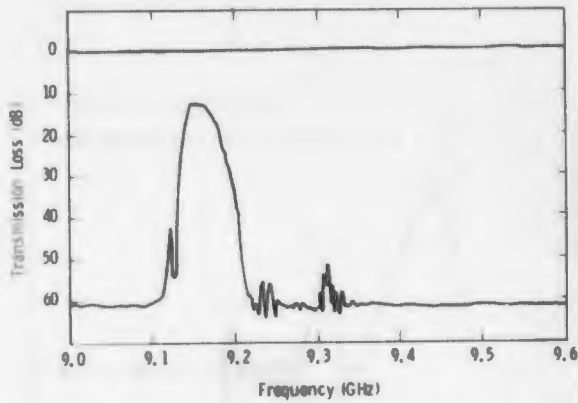


Figure 14. Measured transmission loss as a function of frequency for same parameters as Figure 13 except ends of YIG were reflecting and 0.31 mm from the transducers and 18 aluminum strips 364Å thick evaporated onto the YIG surface.

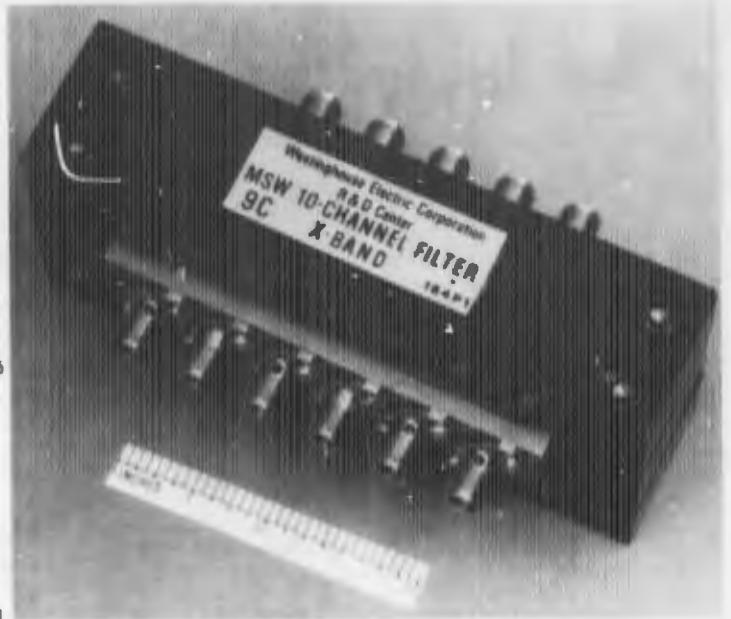


Figure 15. 10-channel filter.

0.31mm. Now the $m = 3$ mode is approximately 40dB down on the $m = 1$ mode which is reasonably symmetrical in passband shape.

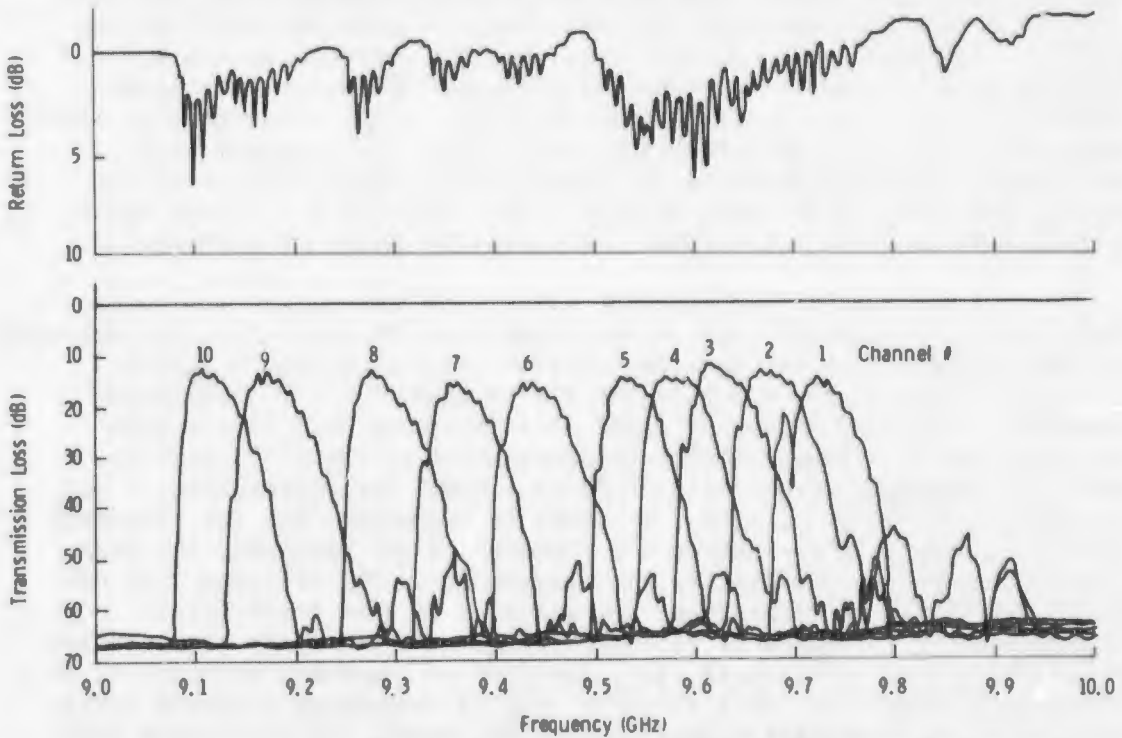


Figure 16. Measured transmission loss and return loss from input for 10-channel filter.

10 YIG strips each 23 μ m thick, 1mm wide and 6.65mm long were positioned as shown in figure 12. The spacing from the end of the YIG strip to the transducer was 0.31mm and the path length \sim 5.4mm. The YIG strips were spaced from the transducer by glass slides 160 μ m thick. The assembled device, complete with bias magnet, is shown in figure 15 and the measured transmission and return loss for all 10 channels as a function of frequency is shown in figure 16. In these results the out of band $m = 3$ responses are higher than desired probably due to a reduction in the number of thin aluminum strips to 15 without any compensating change in thickness. The non-uniform spacing of the pass band center frequencies is due to the non-linear variation in bias field along the device length. In addition, variations in the spacing of the ends of the YIG from the transducers resulted in changes in the pass band shapes. In spite of these shortcomings, which are all potentially correctable, a general technique for obtaining multichannel filter operation has been demonstrated. In addition it has been shown that a degree of control of the pass-band shape can be obtained with simple single element microstrip transducers. Further control may be possible with relatively simple multi-element transducers.

Conclusions

The successful operation of these 4 devices demonstrates that MSW can indeed perform functions at X-band equivalent to those performed by SAW at VHF. Further development is required on all the devices before their performance is sufficient for systems use but they show sufficient promise that they warrant consideration for future radar and ecm systems applications.

REFERENCES

1. "Magnetic Surface Wave Device Technology" J. D. Adam, M. R. Daniel, T. W. O'Keeffe and P. R. Entage. Final report on Contract Number F33615-77-C-1068; AFSC Aeronautical Systems Division, Wright Patterson AFB, OH 45433.
2. Z. M. Bardai, et. al. AIP Conference Proc. No. 34, 268, (1977).
3. P. R. Entage, Journal of Applied Physics, 49, 4475, (1980).
4. Michael R. Daniel et al, IEEE Ultrasonics Symposium Proc. 806 (1979) IEEE Cat. No. CH1472-9/79/0000-806.
5. J. C. Sethares, et al, Electronics Letter, 16, 825, (1980).
6. "Magnetostatic Wave Propagation in YIG double films", Michael R. Daniel and P. R. Entage, 1981 Microwave Magnetics Technology Workshop Proceedings.
7. T. W. O'Keeffe et al, IEEE Ultrasonics Symposium Proceedings, 522 (1980), IEEE Cat. No. 0090-S607/80/0000-0522.

8. YIG Device Catalogue, Watkins Johnson Co., (1978).
9. H. L. Glass et al, Materials Research Bulletin, 12, 755, (1977).
10. J. P. Casters, IEEE Trans., MAG-14, 826, (1978).
11. J. D. Adam et al, Journal of Applied Physics, 49, 1797 (1978).
12. Manufactured by Brown Boveri-Recoma Inc.
13. "The Effects of Width Modes in Magnetostatic Forward Volume Wave Propagation", J. D. Adam, 1981 Microwave Magnetics Technology Workshop Proceedings.

